Electronic Supplementary Material (ESI) for Journal of Materials Chemistry A.
This journal is © The Royal Society of Chemistry 2014

Graphitic Carbon Nitride Nano-Emitters on Silicon: a Photoelectrochemical Heterojunction Composed of Earth-Abundant Materials for Enhanced Evolution of Hydrogen

M. Lublow [a,b], A. Fischer [a], C. Merschjann[c], F. Yang[b], Th. Schedel-Niedrig[b], J.-F. Veyan[d], and Y. J. Chabal[d]

[a]Technical University Berlin, Institute of Chemistry, Germany.
[b]Helmholtz-Zentrum Berlin für Materialien und Energie, Institute Solar Fuels, Germany.
[c]Universität of Rostock, Institute of Physics, Germany.
[d]University of Texas at Dallas, Department of Materials Science and Engineering, USA.

Supporting Information

1. Experimental details

1.1 XeF_2 dry etching of silicon

An all-aluminum custom-made three-stage reaction cell was used, coupled to an FTIR Nicolet 6700 interferometer for both in situ and real-time infrared absorption spectroscopy. In an additional storage chamber, XeF_2 is stored as a powder in a small, sealed stainless steel storage vessel. The first stage is a clean expansion chamber to isolate the pure XeF_2 in its gas phase. The second stage is the reactor equipped with two KBr windows, allowing the IR beam to penetrate and exit the enclosure. This stage is used to realize a controlled XeF_2 gas pressure (~ 3 Torr). The silicon samples were exposed to the gaseous XeF_2 in stage 3. In our sample preparation, two etching cycles were applied. An etching cycle is defined as follows. The reactor and the sample compartment are fully pumped to remove any product gases (from an earlier cycle). XeF_2 is then first introduced into stage 2 at the desired pressure. When the XeF_2 pressure is stable, the gate valve, decoupling the sample from stage 2, is opened and the sample is exposed to XeF_2. The cycle ends when all XeF_2 has been consumed and no more product gases are generated. Prior to the described treatment, all silicon samples were pre-etched by HF(50%) for 30 s in order to remove the native SiO_2 layer.

1.2 g-C_3N_4 preparation, preparation route 1

Dicyandiamide ($C_2N_4H_4$) precursors (99%) were obtained from Sigma Aldrich. Polymeric carbon nitride (g-C_3N_4) films were synthesized by thermal polycondensation of $C_2N_4H_4$ powders at a temperature of 550°C under inert nitrogen gas atmosphere (nitrogen purity > 99.99%). The polycondensation process was carried out employing a heating rate of 20°C per minute. After reaching the maximum temperature of 550°C the samples were kept at this temperature for 30 min.

1.3 g-C_3N_4 preparation, preparation route 2

The polycondensation process was interrupted at a temperature where the transition of the intermediates melamine to melem occurred (between 210°C and 400°C). Using a spatula, the liquid melamine was uniformly spread across the silicon supports. During this time the polycondensation chamber was partially exposed to ambient air while the nitrogen flow into the chamber was maintained.

1.4 Chemical etching by HF (50%)

The C_3N_4/p-silicon samples were immersed into a beacher containing 20 ml HF (50%) for incremented times of 10, 20 and 30 s, subsequently rinsed with ultra-pure water (18 MΩcm) and dried by nitrogen.

1.5 Photoelectrochemical measurements

Photocurrent measurements were performed using a Biologic potentiostat. The setup of the electrochemical cell consisted of a Teflon cell body and three electrodes, i.e. the working electrode (bare silicon, g-C_3N_4/silicon and g-C_3N_4/FTO electrodes, respectively), a platinum wire as counter electrode and a Ag/AgCl electrode as reference electrode, being in contact with saturated KCl [0.197 V vs. the normal hydrogen electrode (NHE)]. For illumination, a tungsten–iodine (W–I) lamp was used (Fiber Lite MI-150 from Dolan–Jenner Industries) with a light intensity of 100 mW cm^{-2} (corresponding to 1 sun, i.e. AM 1.5 G condition). 1 M sulfuric acid (H_2SO_4) solution (pH 0) was used as electrolyte. A back contact between the silicon supports and a steel back-plate of the electrochemical cell was realized by an InGa eutectic. The g-C_3N_4/FTO electrodes were contacted by two steel clips positioned onto g-C_3N_4-free FTO areas. Prior to electrochemical measurements, the electrolyte was degassed by nitrogen bubbling (purity > 99.999%) for five minutes.

1.6 Surface analysis by atomic force microscopy and scanning electron microscopy

Tapping mode atomic force microscopy (TM-AFM) was carried out using a Nanoscope IIIa, (Digital Instruments) with high resolution AFM tips (tip radius about 4 nm). Scanning electron microscopy (SEM) was performed with a Leo 1530 (Zeiss, Germany). Images recorded in the "InLens" mode, as annotated in the respective pictures, were obtained at a detection angle of 90° with respect to the surface normal. Images recorded in the "SE2" mode were obtained at a detection angle of approximately 45°.

1.7 Mass spectroscopic detection of evolving hydrogen

Differential electrochemical mass spectroscopy (see Figs. S6 – S8) employed a two-stage vacuum system. Evolving gas was pumped through a first stage (initial pressure 10^{-4} mbar, operational pressure 1 – 3 x 10^{-3} mbar) and analyzed by a quadrupol mass spectrometer (initial pressure 10^{-9} mbar, operational pressure about 10^{-7} mbar). Prior to the measurements, the 1M H_2SO_4 electrolyte was purged by N_2. The measurements are of qualitative nature only. Particularly at high current densities, not all evolving gas could be transferred towards the detection system.

2. Film surface and thickness analysis

TM-AFM analysis demonstrates a pronounced surface corrugation of the XeF_2 dry etched silicon supports with etch pits extending into the substrates by about 140 nm (see Fig. S1).

After polycondensation of g-C_3N_4 films on the silicon supports and subsequent etching in HF (50%), according to preparation route 1, remnant g-C_3N_4 sheets cover the side-walls of these etch pits (see Fig. S2). The thickness deduced from the SEM image in Fig. S2 appears not to exceed a few 10 nm as indicated by the two yellow arrows. Thickness analysis of the corresponding nano-lamellae (see Fig. S3) is more difficult to achieve since the entire surface area of the silicon support is covered. At sites where the nano-lamellae appear to be bent upwards (towards the detection unit of the microscope) thicknesses of a few 10 nm appear likely. In Fig. S3, such a region is marked by two yellow arrows.

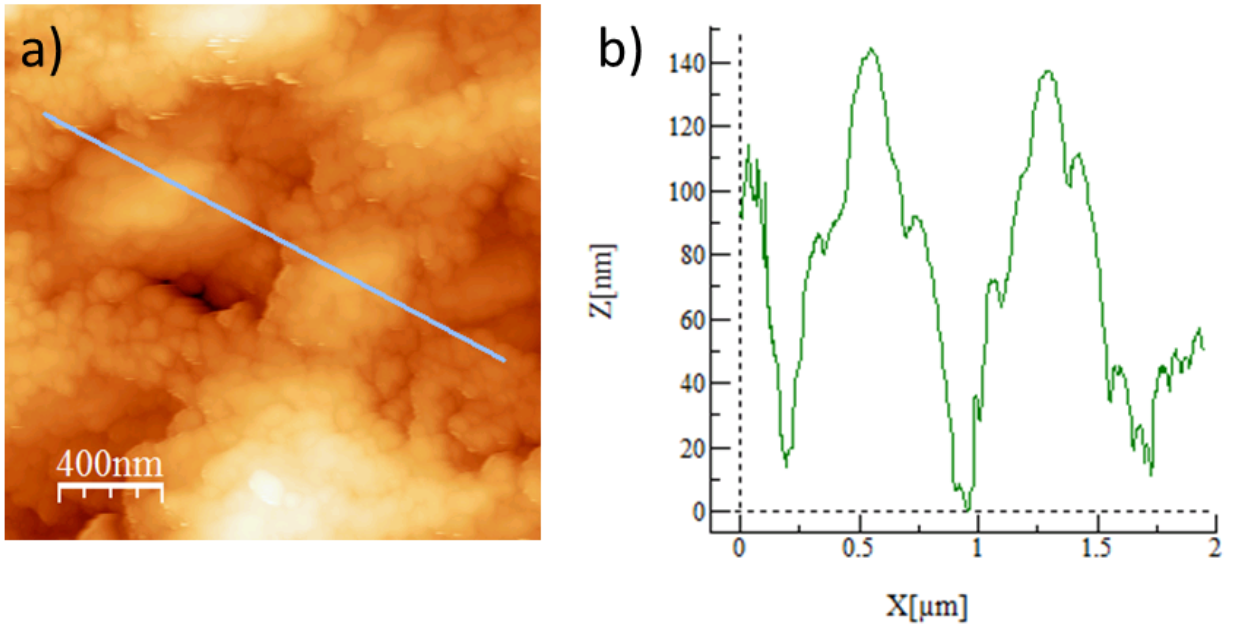

Fig. S1: Surface morphology of the XeF_2 dry etched silicon support investigated by tapping-mode atomic force microscopy (TM-AFM). (a) TM-AFM microscopy image. (b) Surface profile along the blue line indicated in (a).

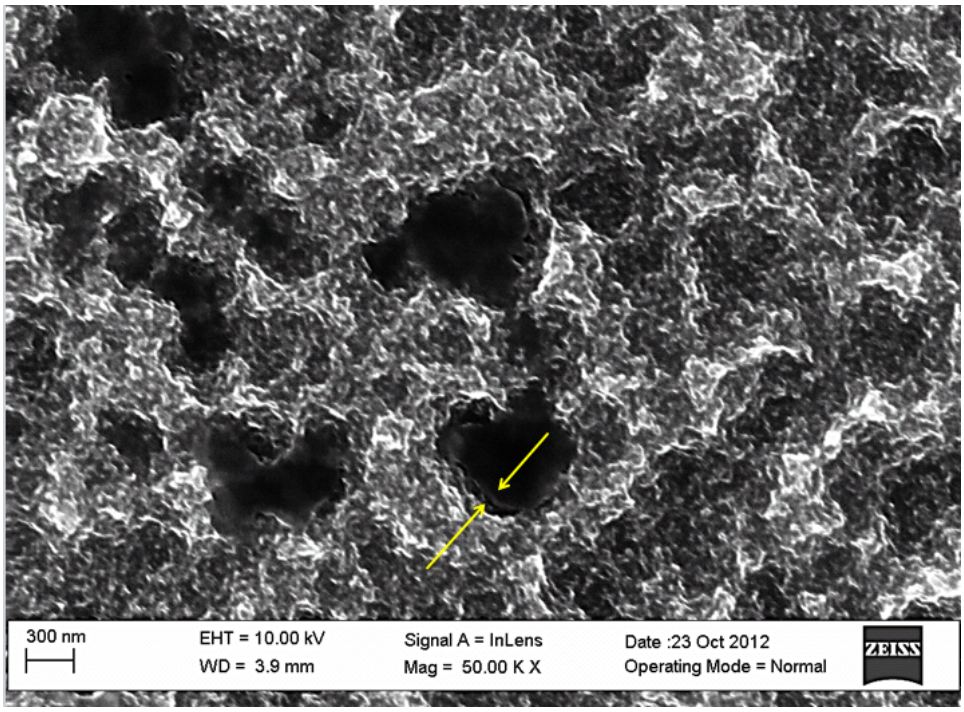

Fig. S2: SEM analysis of the surface morphology after polycondensation of g-C_3N_4 on XeF_2 dry etched silicon and after subsequent etching in HF (preparation route 1). Yellow arrows indicate the thickness of remnant g-C_3N_4 nano-sheets covering the side-walls of the pores, obtained by XeF_2 etching.

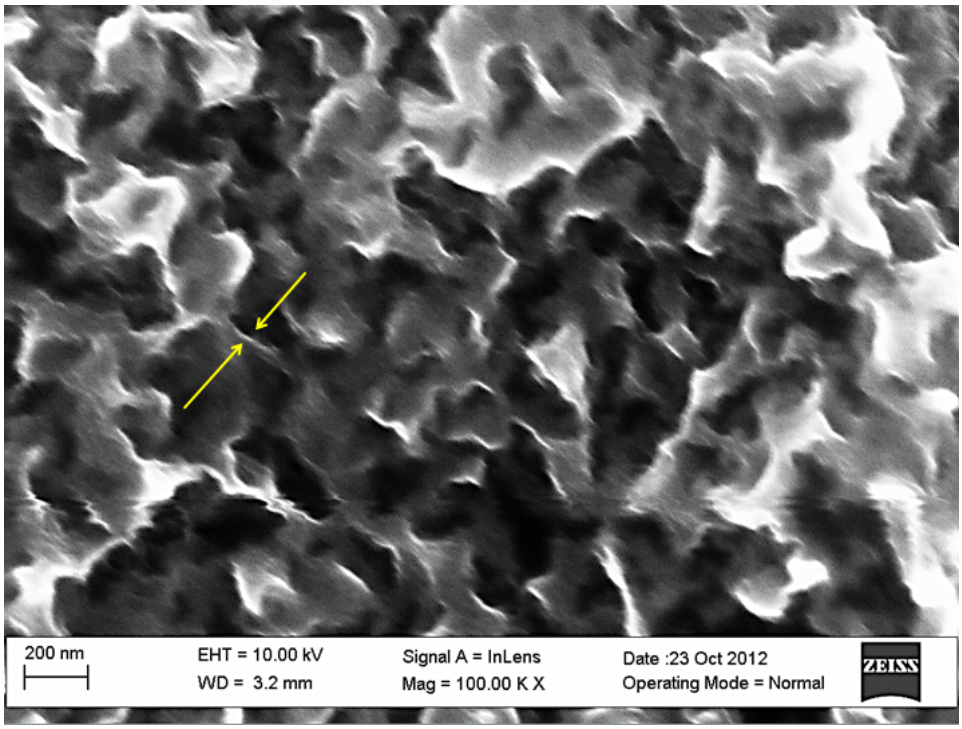

Fig. S3: SEM analysis of the surface morphology after polycondensation of g-C_3N_4 on XeF_2 dry etched silicon with intermediate smoothening of the liquid melamine and subsequent etching in HF (preparation route 2). Yellow arrows indicate the thickness of g-C_3N_4 nano-lamellae.

3. Photoelectrochemical behavior

3.1 g-C3N4 on FTO supports after mechanical thinning

For comparison, g-C_3N_4 films were prepared on non-photoactive fluorinated tin oxide (FTO) supports. The as-deposited films did not show any photoactivity. After mechanical thinning by abrasive paper, photocurrent densities at the redox potential of hydrogen evolution were observable but did not exceed about 1 μAcm^{-2}. A marked contribution of g-C_3N_4 ultra-thin films to the corresponding photocurrent behavior of the Si/g-C_3N_4 heterojunctions can therefore be excluded. In Fig. S4, SEM surface analysis and photoelectrochemical behavior are depicted.

The photocurrent behavior of g-C_3N_4 nano-sheets on p-Si(100) substrates is demonstrated in Fig. S5 for three different light intensities. The dark current density (not shown here) reaches only a few μAcm^{-2}. Saturation photocurrents below approximately -0.6 V form therefore a horizontal line. The photoelectrochemical efficiency appears comparable to the corresponding efficiency of nano-lamellae on p-Si (see manuscript, Fig. 4).

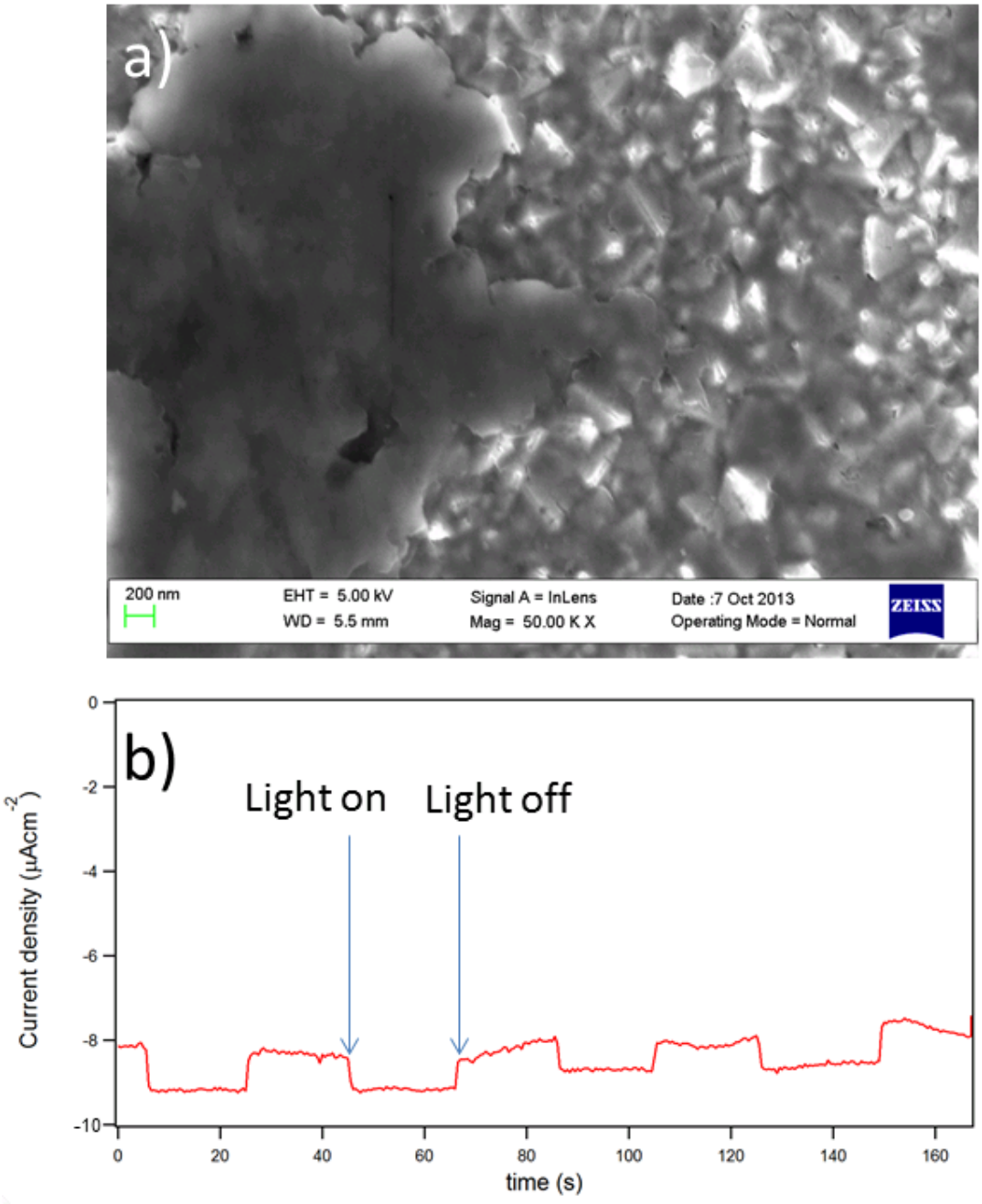

Fig. S4: SEM surface analysis (a) and electrochemical response to illumination (b) of g-C_3N_4 deposited on FTO supports. The g-C_3N_4 layer was mechanically thinned by abrasive paper. In (a) a thickness variation across the FTO surface is recognizable with regions of approximately 100 nm thickness (left) and regions with a surface coverage of a few 10 nm. Photocurrents at the redox potential for hydrogen evolution in (b) do not exceed 1 µAcm^{-2}.

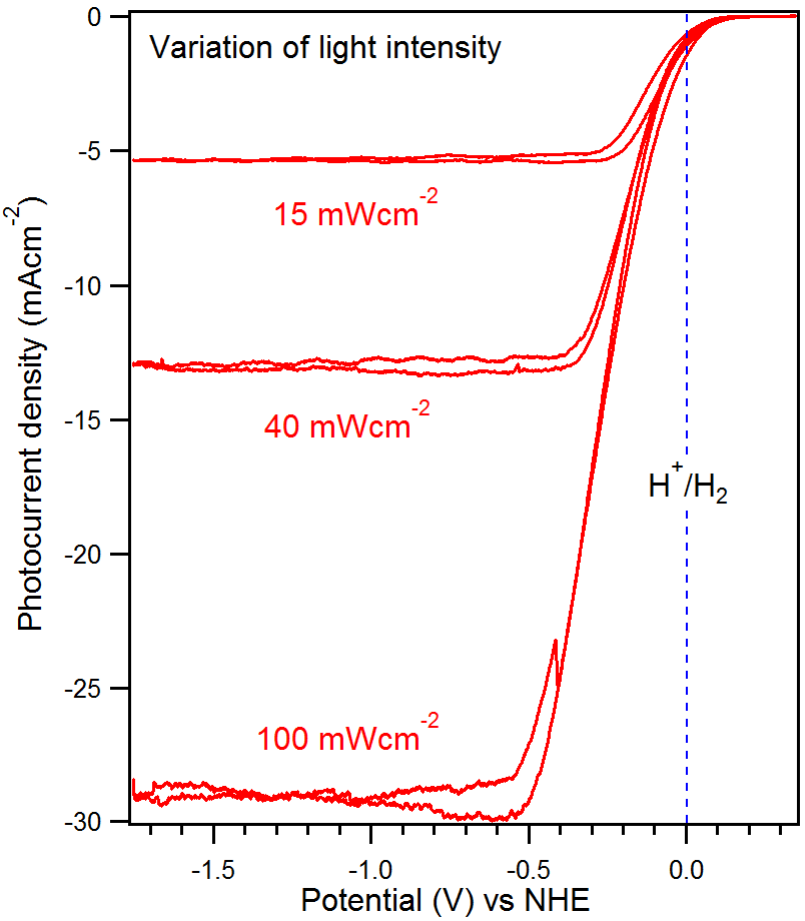

Fig. S5: Photoelectrochemical behavior of g-C_3N_4 nano-sheets on p-Si(100). Light intensities were varied between 15 and 100 $mWcm^{-2}$. The heterojunction operates as pure photoelectrode. Dark current contributions remained below 10 μAcm^{-2}.

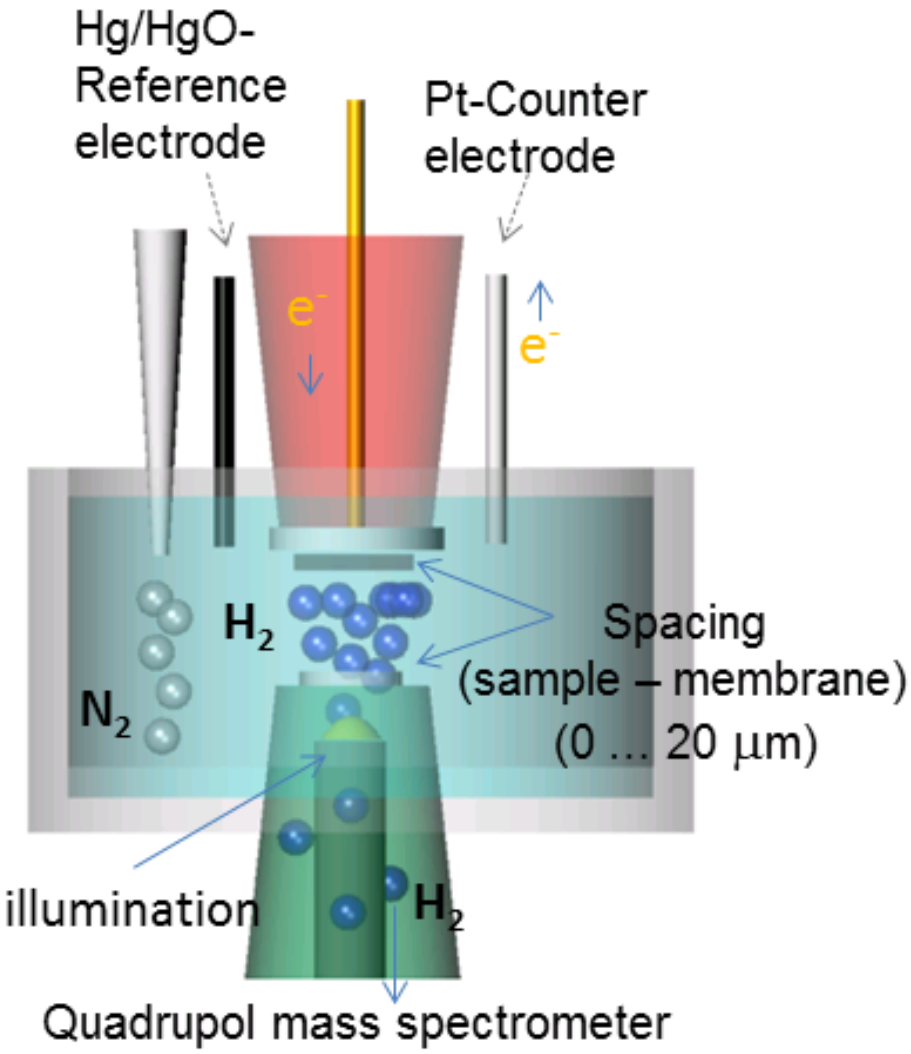

Figure S6. Schematic view of the setup for DEMS measurements. The electrochemical cell was operated in a three-electrode arrangement with Pt-counter and Hg/HgO-reference electrode. Prior to the measurements, the 1M H_2SO_4 electrolyte was purged by N_2 for removal of dissolved hydrogen. The purging was continued during operation. The variable distance between sample and gas-permeable membrane was set to nominally zero in order to achieve maximum sensitivity with respect to H_2-detection. A potential shift of about 200 mV was thereby caused. Particularly at high current densities, not all evolving gas could be transferred through the detection system.

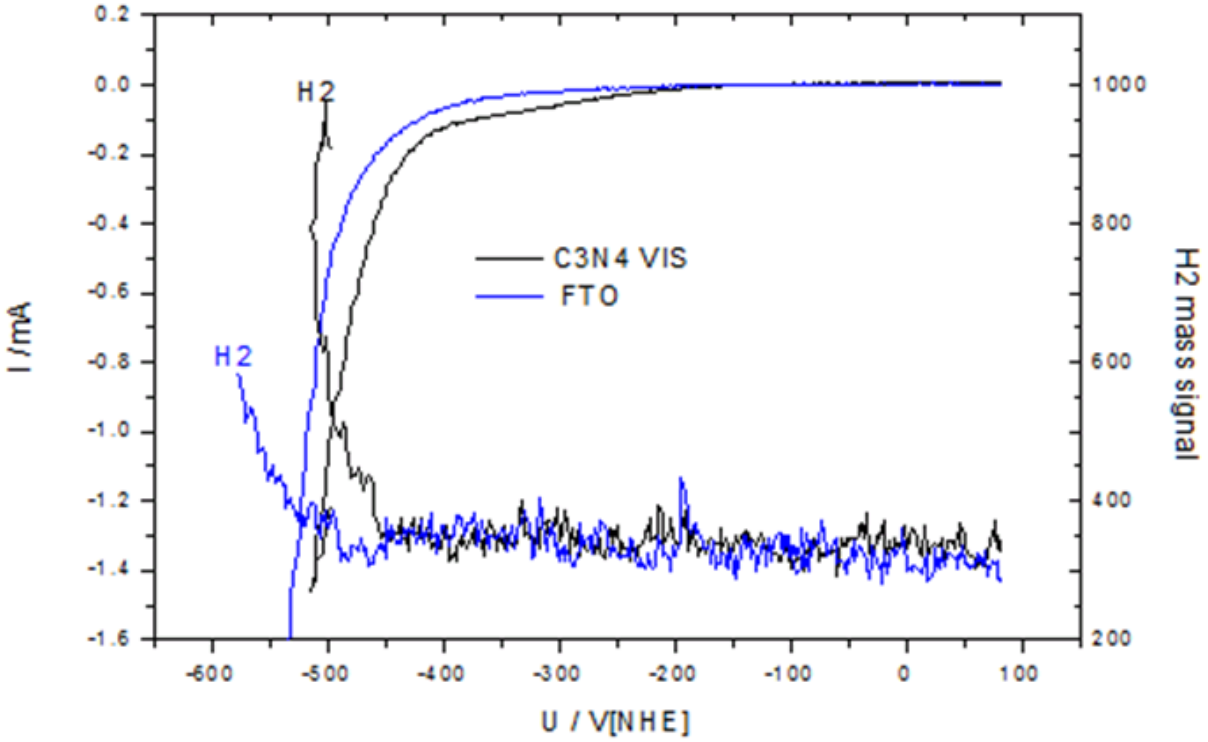

Figure S7. DEMS measurements: comparison of H_2 evolution at the FTO and C_3N_4/FTO electrode, respectively. H_2 evolution at the C_3N_4/FTO electrode under AM1.5 conditions (black curves) shows only small photoelectrocatalytic improvements in comparison to the bare FTO substrate (blue curves). Measurements were carried out in 1M H_2SO_4.

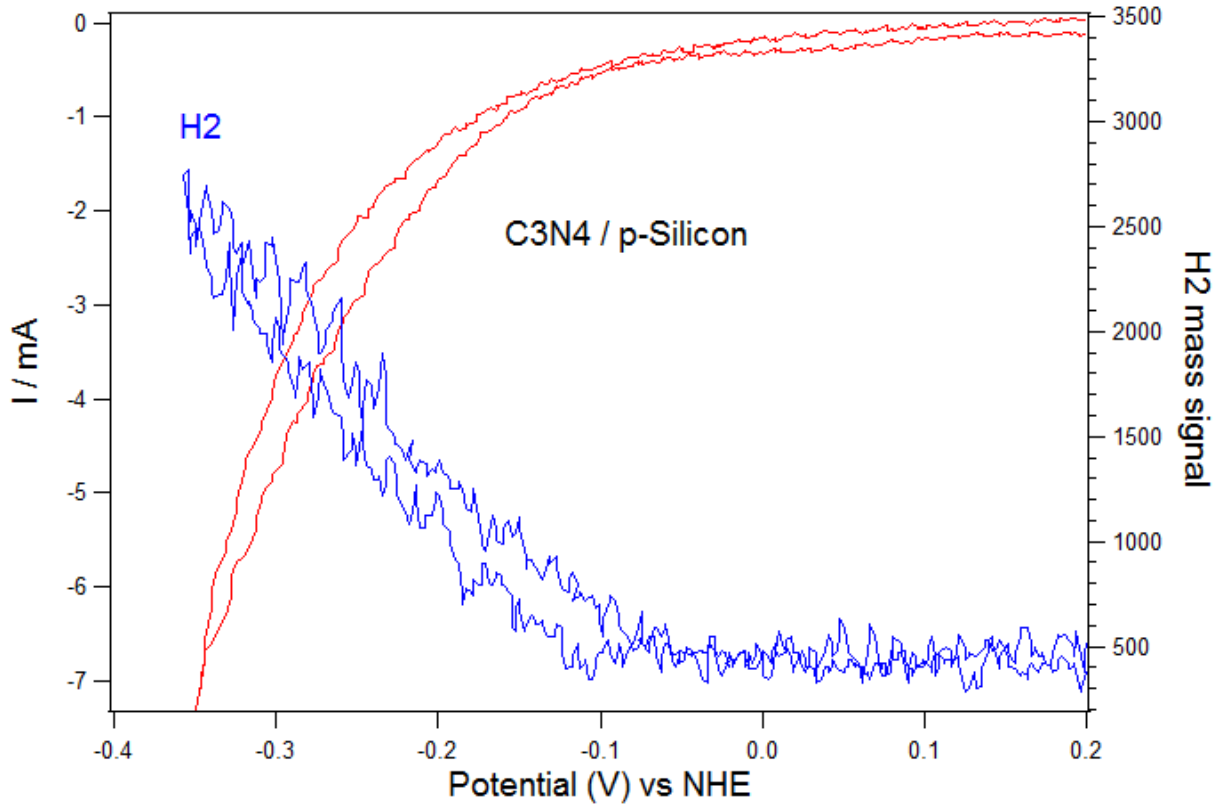

Figure S8. DEMS measurements: evolution of H_2 at the C_3N_4/p-silicon electrode (nano-lamellae). The mass spectroscopic signal confirms the evolution of H_2 at the surface of the C_3N_4/p-silicon electrode (nano-lamellae) heterojunction. Measurements were carried out in 1M H_2SO_4. Illumination intensity corresponds to AM1.5 conditions. In comparison to measurements without gas-permeable membrane a shift of the onset potential by about 200 mV was observed due to strong diffusion limitation.